

Submitted to *Astrophys. J.*

OXYGEN ABUNDANCE DETERMINATION IN VERY METAL-POOR GIANTS: PERMITTED O I LINES VERSUS FORBIDDEN [O I] LINES

YOICHI TAKEDA

Institute of Astronomy, The University of Tokyo, Mitaka, Tokyo, Japan 181-0015

takedayi@cc.nao.ac.jp

MASAHIKE TAKADA-HIDAI

Research Institute of Civilization, Tokai University, 1117 Kitakaname, Hiratsuka, Kanagawa, Japan 259-1292

hidai@apus.rh.u-tokai.ac.jp

SHIZUKA SATO

Department of Aeronautics, School of Engineering, Tokai University, 1117 Kitakaname, Hiratsuka, Kanagawa, Japan 259-1292

shizuka@apus.rh.u-tokai.ac.jp

WALLACE L. W. SARGENT and LIMIN LU

Astronomy Department, California Institute of Technology, Mail Stop 105-24, Pasadena, CA 91125

wws@astro.caltech.edu

THOMAS A. BARLOW

Infrared Processing and Analysis Center, California Institute of Technology, Mail Stop 100-22, Pasadena, CA 91125

tab@ipac.caltech.edu

and

JUN JUGAKU

Research Institute of Civilization, 2-29-3 Sakuragaoka, Tama-shi, Tokyo, Japan 206-0013

jugakujn@cc.nao.ac.jp

ABSTRACT

The abundance of oxygen was determined for selected very metal-poor G–K stars (six giants and one turn-off star) based on the high S/N and high-resolution spectra observed with Keck HIRES in the red through near-IR region comprising the permitted O I lines (7771–5, 8446) along with the [O I] forbidden line at 6363 Å. It turned out that both the abundances from the permitted line features, O I 7771–5 and O I 8446, agree quite well with each other, while the forbidden line yields somewhat discrepant and divergent abundances with a tendency of being underestimated on the average. The former (7773/8446) solution, which we believe to be more reliable, gives a fairly tight [O/Fe] vs. [Fe/H] relation such that increasing steadily from $[O/Fe] \sim 0.6$ (at $[Fe/H] \sim -1.5$) to $[O/Fe] \sim 1.0$ (at $[Fe/H] \sim -3.0$), in reasonable consistency with the trend recently reported based on the analysis of the UV OH lines. We would suspect that some kind of weakening mechanism may occasionally act on the formation of [O I] forbidden lines in metal-poor stars. Therefore, [O I] lines may not be so a reliable abundance indicator as has been generally believed.

Subject headings: Galaxy: evolution — stars: abundances — stars: atmospheres — stars: Population II

1. INTRODUCTION

The hot controversy on the trend of the oxygen abundance in very old metal-deficient stars is one of the most interesting topics in the field of stellar spectroscopy as well as Galactic chemical evolution. (See, e.g., Carretta, Gratton, & Sneden 2000 and references therein for overviewing the current status of this problem.)

The essential point of the argument is, shortly speaking, how the [O/Fe] ratio behaves itself toward the regime of very low metallicity, say, down to $[Fe/H] \sim -3$. Admittedly, it seems to have been almost established that [O/Fe] increases from ~ 0.0 ($[Fe/H] \sim 0$) to ~ 0.4 ($[Fe/H] \sim -1$) for stars of disk population. However, when stars of old halo population are concerned, we are wondering whether [O/Fe] shows a nearly flat plateau at $[O/Fe] \sim +0.5$ (“plateau” trend) or it continues to increase steadily up to $[O/Fe] \sim +1$ (“steady increase” trend), as [Fe/H] decreases from ~ -1 down to ~ -3 .

From observational point of view, this problem is closely connected with the technical details of abundance determination; i.e., especially important is which of the spectral lines to be adopted. In the present case of late-type stars, the candidates of the lines used for O-abundance determination are roughly divided into three groups :

- (1) O I permitted lines (e.g., 7771–5 triplet)
- (2) [O I] forbidden lines (6300/6363 doublet)

(3) OH lines in the UV region of 3100–3200 Å

Among these the [O I] forbidden lines (originating from the ground level) have so far been regarded as being the most reliable abundance indicator because of its low T_{eff} sensitivity along with the certain validity of the LTE assumption, in contrast to the high-excitation permitted lines which are T_{eff} -sensitive and more or less affected by a non-LTE effect.

Generally speaking, there seems to have been an implicit consensus that the “plateau” trend probably represents the truth, partly because it is suggested from the analysis of [O I] 6300 forbidden line, though with a rather large scatter (see, e.g., Fig. 11 in Timmes, Woosley, & Weaver 1995). In addition, the fact that this “flat” behavior is consistent with the trend posed by other α -elements (Mg, Si, Ca, Ti) may have substantiated this view. Namely, it is reasonably explainable based on the standard theory of Galactic chemical evolution. That is, a steady enrichment of α -elements along with Fe with a constant α -to-Fe ratio by massive stars via type II SNe (very short time-scale nearly like instantaneous recycling) in the earlier phase of Galactic evolution, and then later type Ia SNe (long time-scale of the order of 10^9 yr) begins to explode to eject Fe, which must have gradually suppressed $[\alpha/\text{Fe}]$ eventually down to the current value.

On the other side, the O I 7771–5 lines were known to imply the “steady increase” trend (see, e.g., Fig. 1 in Bessell, Sutherland, & Ruan 1991, or Fig. 4 in Mishenina et al. 2000), which means that these permitted lines yield higher abundance than that resulted from the forbidden line. Nevertheless, it appears that this tendency has not been taken too seriously compared to the [O I] results for the uneasy problems involved with these lines mentioned above.

Recently, however, Israelian, García López, & Rebolo (1998) and Boesgaard et al. (1999) reported that [O/Fe] clearly increases from $\sim +0.6$ to $\sim +1.0$ as [Fe/H] varies from ~ -1.5 to -3 (just similar to what had been implied by 7771–5 permitted lines) based on their new independent analyses of numerous OH lines in UV, which have sufficient strengths even in extremely metal-poor stars and thus suitable for abundance determination. This “steady increase” trend has thus acquired a special attention as the true [O/Fe] vs. [Fe/H] relation, though this must be quite embarrassing for theoreticians (i.e., theoretical interpretation becomes much harder).

Even so, the problem is still far from being settled, unfortunately. A strong criticism was successively addressed by Fulbright & Kraft (1999), who reinvestigated the atmospheric parameters of two extremely metal-poor stars studied by Israelian et al. (1998) and showed that their large [O/Fe] values ($\sim +1$) can be considerably reduced down to $\sim +0.5$ if the [O I] 6300 line was used, concluding that it is still premature to accept their OH results.

So we are in a quite confusing situation. Which line gives the correct oxygen abundance? [O I] forbidden line? O I permitted lines (which yield the same trend as that given by OH lines)? This topic attracted our attention, since we once confirmed that the oxygen abundances derived from O I 7771–5 lines and [O I] 6300 line do not show any systematic discordance from the analysis of Population I G–K giants (Takeda, Kawanomoto, & Sadakane 1998a).

Consequently, we decided to conduct a detailed analysis of selected seven very metal-deficient

stars ($-3 \lesssim [\text{Fe}/\text{H}] \lesssim -1.5$) based on the high-quality spectra observed with Keck HIRES, in an attempt to compare the abundances of oxygen derived from the permitted O I lines (7771–5, 8446) and forbidden [O I] lines (6363, 6300) with each other, as well as to settle which of the [O/Fe] trend is more likely. We will show later that the former “permitted” O I lines are probably a more reliable abundance indicator rather than the forbidden [O I] lines, lending support for the “steadily increasing” trend of [O/Fe].

2. OBSERVATIONAL DATA

2.1. Observations

The spectroscopic observations were carried out for six HD-numbered very metal-deficient stars (five G–K giants and one turn-off star in the metallicity range of $-3 \lesssim [\text{Fe}/\text{H}] \lesssim -1.5$) in the seasons of 1997 May and 1999 November using the High Resolution Echelle Spectrograph (HIRES; Vogt 1994) of the Keck I Telescope. Basic observational data of the program stars are given in Table 1.

2.2. Data Reduction

The data were reduced with the HIRES Automated Reduction (HAR) software package developed by T. A. Barlow. This package converts the two-dimensional echelle raw data to one-dimensional wavelength-calibrated spectrum of each order with full processings of bias subtraction, flat fielding, cosmic-ray correction, sky subtraction, and dispersion correction. The multiple calibrated spectra were coadded using the IRAF package *scombine* and then normalized to continuum level of unity using the IRAF package *continuum* for 1997 May data and the HAR package *xplot* for 1999 November data.

The wavelength range of the spectrum is $6330 \text{ \AA} \lesssim \lambda \lesssim 8760 \text{ \AA}$, which comprises the lines of [O I] 6363, O I 7771–5, and O I 8446. Since we tried to cover the long-wavelength range up to 8760 Å (because of our intention of observing special spectral lines such as those of sulfur), we were obliged to set the short-wavelength limit at 6330 Å. Consequently, we had to abandon using the [O I] 6300 line.

2.3. CS 22892-052

Regarding CS 22892-052, the well-known carbon-rich very metal-poor star with excesses of neutron-capture elements (cf. Sneden et al. 1994), we used the Keck HIRES spectrum which was kindly reduced and provided by M. Kuchner (private communication) covering the wavelength range of $5340 \text{ \AA} \lesssim \lambda \lesssim 7770 \text{ \AA}$. Unfortunately, the signal-to-noise ratio of this spectrum is considerably

poor (120–140) compared to those of other six stars. Since the long-wavelength limit is just on the position of O I 7771–5 triplet, only the shortest-wavelength component (at 7771.94 Å) of the three could be used. Note also that the [O I] 6300 line was usable in addition to [O I] 6363, while the O I 8446 line is not included in this spectrum.

2.4. Equivalent-Width Measurements

The identification of spectral lines, the selection of blend-free lines usable for abundance determination, and the evaluation of equivalent widths by Gaussian fitting (or by direct integration if necessary) were carried out with the help of the interactive GUI software “SPSHOW”, which was developed by Y. Takeda based on Kurucz’s ATLAS/WIDTH code as a multi-purpose tool for stellar spectrum analysis (e.g., synthesizing a theoretical spectrum with any abundance/line-broadening, browsing of observed spectrum to be overplotted, radial-velocity correction by fitting with an appropriate horizontal shift, interactive abundance-determination, equivalent-width measurement, etc.) We measured the equivalent width for all spectral lines as possible (irrespective of the species) as far as being confidently identified and free from blending with other lines. These data were further used for abundance determination as described in §3.2.

3. ABUNDANCE DETERMINATION

3.1. Model Atmospheres

We used Kurucz’s (1993) ATLAS9 line-blanketed model atmospheres, based on which the atmospheric models of individual stars were constructed by interpolation in terms of T_{eff} , $\log g$, and [X] (metallicity).

Regarding the choice of these parameters, we adopted the values established by Pilachowski, Sneden, & Kraft (1996) if available (HD 44007, HD 165195, HD 175305, HD 184266), since their determinations appear to be reliable, because they were based on careful considerations and checked from various standpoints.

As for HD 84937 and HD 88609, the T_{eff} values were evaluated from $(b - y)_0$ color (0.30 and 0.65), which were taken from the compilation of Hauck and Mermilliod (1998) and corrected for reddening as described below, in the same way as was done by Pilachowski et al. (1996), yielding 6040K and 4440K, respectively. We applied a slight reddening correction (−0.03) corresponding to the E_{B-V} value of +0.04 (cf. Bond 1980; $E_{b-y} = 0.73E_{B-V}$) for HD 88609 to obtain $(b - y)_0$ from the raw $b - y$, while $E_{b-y} = 0$ could be safely assumed for the nearby (81 pc) turn-off star HD 84937. We then computed the $\log g$ values from L (bolometric luminosity), which were derived from Hipparcos data with the bolometric correction estimated from Kurucz’s (1993) theoretical colors, while using the adopted T_{eff} and assuming $0.8 M_{\odot}$ (Pilachowski et al. 1996), and eventually

obtained 4.0 and 0.8, respectively. Comparing such calculated T_{eff} and $\log g$ with the published values compiled by Cayrel de Strobel et al. (1997), which we also consulted for estimating the stellar metallicity, we finally adopted (6100K, 4.0, -2.3) and (4500K, 1.0, -2.7) for $(T_{\text{eff}}, \log g, [\text{X}])$ of HD 84937 and HD 88609, respectively.

Concerning CS 22892-052, we simply used the parameters determined by McWilliam et al. (1995). The finally adopted model parameters for our program stars are given in Table 2.

3.2. Microturbulence and Elemental Abundances

We used the WIDTH9 program written by R. L. Kurucz to determine the elemental abundances, where the gf values compiled by Kurucz (1995) were exclusively used.

Practically, the values of the microturbulence were first established from the equivalent widths of Fe I lines, following the procedure adopted by Takeda (1992), and are given in Table 2. We then determined the abundances of various elements (apart from C and O which were treated specially) from the measured equivalent-widths of spectral lines, with the corresponding atmospheric model and the microturbulent velocity.

The resulting abundances averaged over each of the lines are presented in Table 2. In case where lines of two ionization stages were available, we took their simple mean.

Although the detailed data and results for each line (e.g., the equivalent width, the gf value, and the abundance, etc.) are not shown in this paper, complete tables in a machine-readable form containing all these data are downloadable from the following anonymous ftp site.

```
IP address: 133.11.160.7
directory: /Users/takeda/oxygen2000/tables/
```

We confirmed almost satisfactory accomplishment of the ionization equilibrium between Fe I and Fe II, since the abundance difference (Fe I – Fe II) turned out to be $+0.08$, -0.09 , -0.14 , -0.07 , $+0.17$, $+0.05$, and $+0.06$ (in the same order as in Table 2). Note also that the resulting [Fe/H] values are consistent with the adopted metallicity of the model.

3.3. Oxygen Line Analysis

3.3.1. Non-LTE Calculation

The statistical-equilibrium calculations for oxygen were carried out twice for each star by assuming two input oxygen abundances $[\text{O}/\text{Fe}] = 0$ and 1. See Takeda et al. (1998a) and the references therein for computational details. The resulting departure coefficients and line-source functions were further used to determine the non-LTE oxygen abundance.

3.3.2. CO Molecule Effect

As described in the following, we determine the oxygen abundance from the equivalent widths of oxygen lines or by profile-fitting. Here, there is one thing we should be aware in the present case of late-type stars. Since an appreciable fraction of C and O atoms are combined to form CO molecules, the determination of the abundance of oxygen more or less depends upon that of C along with the O-abundance itself (i.e., the abundance adopted in the model atmosphere). In order to take this effect properly into consideration, we determined the abundance of C for our program stars from [C I] 8727.13 (HD 44007, 88609, 165195) or C I 8335.15 (HD 84937, 175305, 184266), except for CS 22892-052.

Practically, we first determined the O-abundance by assuming $[C/Fe] = 0$ ($[C/Fe] = +1$ only for CS 22892-052; cf. McWilliam et al. 1995). With such determined abundance of oxygen, the abundance of C was evaluated from the equivalent width of the [C I] or C I line. Finally, the oxygen abundance was again computed with this updated C-abundance.

Actually, this whole procedure was repeated twice in order to derive two oxygen abundances $\log \epsilon_0(O)$ and $\log \epsilon_1(O)$, corresponding to two different input oxygen abundances of the model atmosphere, $[O/Fe] = 0$ and $+1$. Then, the final oxygen abundance to be adopted was derived by finding the consistent solution based on these two.

Nevertheless, both C-dependence and the (input) $[O/Fe]$ -dependence were found to be generally insignificant and negligible in most cases (a few hundredths dex at most). The resulting carbon abundances are given in Table 2.

3.3.3. O I 7771-5

The abundances from these well-known high-excitation O I triplet lines (RMT No.1; $\chi = 9.15$ eV) in the quintet system ($3s\ ^5S^o - 3p\ ^5P$) were derived from their equivalent widths. The gf values (and the damping parameters) were taken from Kurucz (1995); i.e., $+0.32$, $+0.17$, and -0.05 for the lines at 7771.94, 7774.17, and 7775.39 Å, respectively. The results are given in Table 3, where the mean of the non-LTE abundances over the components, $\langle \log \epsilon_{7773} \rangle$, is also presented. (We will regard this $\langle \log \epsilon_{7773} \rangle$ as being the standard oxygen abundance to be adopted.) The theoretical spectrum computed with this $\langle \log \epsilon_{7773} \rangle$ are compared with the observed one for each star in Figure 1, where we can confirm that the fit is quite satisfactory.

In the case of HD 184266, we found that consistency of the abundances for these three components could not be attained with the use of $\xi = 2.2$ km s $^{-1}$, which was derived from Fe I lines (§3.2). We thus adopted the value of 5.1 km s $^{-1}$ (the best-fit value established by profile-fitting; cf. §6.1 of Takeda & Sadakane 1997) for this star. This problem will be discussed further in §4.1.

3.3.4. O I 8446

In contrast to the famous O I 7771–5 triplet, this similar high-excitation O I 8446 feature (RMT No.4; $\chi = 9.52$ eV) in the triplet system ($3s\ 3S^o - 3p\ 3P$) has barely been used for oxygen abundance determination, presumably because it is seriously blended with Fe I lines. We thus applied a profile-fitting technique (Takeda 1995a) to the analysis of this O I + Fe I 8446 blended feature, such as was done by Takeda et al. (1998b). The adopted gf values of the O I components (8446.25, 8446.36, and 8446.76 Å) are (-0.52 , $+0.17$, and -0.05) taken from Kurucz (1995), while those of the blended Fe I lines (8446.39 Å, $\chi = 4.99$ eV and 8446.57 Å, $\chi = 4.91$ eV) were the empirical values of (-0.85 and -1.89) determined by Takeda (1995b). The Fe abundance was simultaneously determined along with that of O as far as possible; otherwise, an appropriate value of the Fe abundance corresponding to the metallicity was assigned and fixed. The resulting oxygen abundances are given in Table 3, where the O I equivalent widths [$W_\lambda(O I 8446)$] corresponding to the pure contribution of three O I component lines, which were inversely evaluated by spectrum synthesis while using the established solutions of the oxygen abundance, are also presented. With the equivalent widths of two Fe I lines similarly computed, we found that the estimated fractions of $W_\lambda(O I 8446) / [W_\lambda(O I 8446) + W_\lambda(Fe I 8446.36) + W_\lambda(Fe I 8446.57)]$ turned out to be 81%, 98%, 53%, 72%, and 98%, for HD 44007, HD 84937, HD 165195, HD 175305, and HD 184266, respectively. The theoretically synthesized spectra computed with $\langle \log \epsilon_{7773} \rangle$ are shown in Figure 2.

3.3.5. [O I] 6363/6300

We adopted Kurucz's (1995) gf value for the [O I] forbidden lines ($2p^4\ 3P - 2p^4\ 1D$); i.e., $\log gf = -9.82$ for [O I] 6300.30 ($\chi = 0.00$ eV) and -10.30 for [O I] 6363.78 ($\chi = 0.02$ eV), though the former was usable only for CS 22892-052. The abundance results are given in Table 3, while the theoretical spectra corresponding to $\langle \log \epsilon_{7773} \rangle$ are shown in Figure 3. Note that the abundances for CS 22892-052 (6363 and 6300 lines) and HD 184266 (6363 line) are uncertain, because of the difficulty in measuring their equivalent widths accurately (i.e., line profiles of these lines are not well defined).

4. DISCUSSION

4.1. HD 184266: Importance of Turbulent Velocity

Before discussing the trend of the oxygen abundance, it may be worth paying attention to HD 184266, which shows markedly stronger O I lines (7771–5, 8446) than any other star, in contrast to the remarkable weakness of [O I] 6363 exhibiting a rather ambiguous profile.

As mentioned in §3.3.3, the abundances derived from three components of the O I 7771–5

turned out to be discordant with each other when the microturbulent velocity of 2.2 km s^{-1} (based on Fe I lines) was used (cf. Table 3). The consistency can be accomplished only when this turbulence parameter is considerably raised up to $\sim 5 \text{ km s}^{-1}$. We point out that this is very similar to the situation experienced by Takeda & Sadakane (1997) in their analysis of Population II horizontal-branch star HD 161817 (cf. §6.1 therein), in which they attributed this discrepancy to the depth-dependence of the turbulent velocity field increasing with atmospheric height

In fact, similar tomography on ξ as was done by Takeda & Sadakane (1997) revealed that two groups of Fe I lines of different χ (lower excitation potential) lead to discrepant values for the ξ value of HD 184266; i.e., 2.3 km s^{-1} with $\langle \log \tau \rangle \sim -0.6$ ($0 \text{ eV} \leq \chi < 4 \text{ eV}$) and 1.8 km s^{-1} with $\langle \log \tau \rangle \sim -0.4$ ($4 \text{ eV} \leq \chi$), indicating a tendency of upward-increasing turbulence. That such a similar phenomenon takes place in the atmosphere of both stars becomes even convincing when we recall HD 184266 is considered to be a horizontal-branch star (i.e., just same as HD 161817) as judged from its position in the HR diagram (cf. Fig. 3 in Pilachowski et al. 1996). Hence we may state that the atmospheric turbulent velocity field in these horizontal-branch stars grows with an increase in height, significantly affecting the strength of such high-excitation O I lines, because they become fairly strong due to relatively high T_{eff} and tend to form higher in the atmosphere.

It is not clear whether such a phenomenon has something to do with the metal-deficiency. Yet, the recent work by Gadun & Ploner (1999) is interesting in this connection, since their calculation indicates that a decrease in metallicity causes the following effects in stellar atmospheres.

- A growth of granulation contrast.
- A growth of atmospheric oscillation.
- An increase of temperature variation in the upper photosphere.
- Size of granules tends to shift toward smaller scales.

Accordingly, we had better pay attention to the treatment of turbulent velocity fields in the atmosphere of metal-poor stars more seriously, at least when saturated lines are concerned.

4.2. Permitted vs. Forbidden Lines

We now discuss the main topic of this paper; i.e., comparison of the oxygen abundances derived from different lines.

As can be seen from Figure 4, the abundances derived from both permitted line features of high excitation (O I 7771–5 and O I 8446) are in remarkable agreement with each other, which can be also intuitively confirmed from Figure 2. This means that these two abundances may be regarded as being essentially equivalent, and that O I (+ Fe I) 8446 is practically usable for oxygen abundance determination supplementing O I 7771–5.

On the other hand, the case of the forbidden line ([O I] 6363 or 6300) is more complicated. What we notice from Figure 4 is the large scatter in the 6363(6300) vs 7773 correlation. More precisely, while a good agreement is observed for HD 165195 and HD 175305, the forbidden [O I]

line tends to yield lower abundance (typically by 0.3–0.4 dex) than those determined from the permitted O I lines for other stars.

According to Table 3, if the T_{eff} of the model atmosphere were increased (say, by ~ 200 K), it would be possible to bring them into consistency, while the effect of changing $\log g$ acts in the same direction for both O I and [O I] lines. Yet, we would consider it rather unlikely that the T_{eff} values of our model atmospheres are correct for some stars on the one hand but not for others on the other, since our adopted T_{eff} scale is based on a consistent system of Pilachowski et al. (1996) (cf. §3.1).

Hence, we regard this discrepancy as being real, in the sense that it is unlikely to be attributed to any systematic error in abundance determination. Accordingly, in contrast to Population I G–K giants where the abundances from O I 7773 lines and [O I] 6300 do not show any systematic discordance (Takeda et al. 1998a), it may be stated that “*metal-poor Population II* G–K giants tend to exhibit abundance discrepancy between these two O I and [O I] lines, though this does not necessarily always happen (i.e., there are surely cases where the consistency is achieved).”

4.3. [O/Fe] vs. [Fe/H] Relation

The resulting [O/Fe] vs. [Fe/H] correlation for O I 7771–5 and [O I] 6363(6300) is depicted in Figure 5, where Israelian et al.’s (1998) results based on the OH lines are also shown for comparison. It can be seen from this figure that the [O/Fe] values from O I 7771–5 lines are reasonably consistent with the OH results showing a “steady increase” trend, while those from [O I] forbidden lines tend to lie below the O I or OH plots by several tenths dex *with a considerably large scatter*. In any case, we have reconfirmed the observational disagreement between the [O/Fe] vs. [Fe/H] relation derived from O I and [O I] lines mentioned in §1.

Then, which represents the truth? We have a preference for the O I permitted lines (7771–5/8446), because they show a clean trend consistent with that exhibited by OH lines. The large diversity of the [O/Fe] values indicated by [O I] lines gives us a feeling that these forbidden lines may be unreliable. Consequently, we conclude that the [O/Fe] vs. [Fe/H] relation for metal-poor stars has the “steady increase” trend, based on our permitted O I lines (7711–5/8446) analysis, lending support for the OH results reported by Israelian et al. (1998) and Boesgaard et al. (1999).

Turning our attention to other recent works, we note that Mishenina et al. (2000) also arrived at the same conclusion as ours based on their non-LTE analysis of the permitted O I 7771–5 triplet, as suggested by previous works (cf. §1). However, there are reports that even the permitted O I lines yield the “flat”-like trend similarly to [O I] lines (e.g., Carretta et al. 2000; Fig. 1 in Gustafsson 1999). The reason for this discordance is not clear; further observational work on a much larger sample of very metal-poor stars and analysis in a fairly consistent system will be needed until this confusion is finally settled.

4.4. Weakening of [O I] line?

Our choice (for the preference of O I and OH lines) naturally means that the abundances from [O I] lines tend to be erroneously underestimated for some reasons. What has happened to these forbidden lines?

We suspect that this line may often suffer with an appreciable weakening in a non-classical way. As a matter of fact, the possibility of such a weakening was once remarked by Langer (1991), who proposed a model that the absorption trough of the low-excitation [O I] forbidden line may be filled with the [O I] emission from the surrounding nebulosity, thus leading to a weakening of the line. In this connection, it is interesting to refer to the [O I] 6363 line of HD 184266, which shows a large O I vs. [O I] discordance amounting to ~ 0.5 dex (cf. Table 3). Let us pay attention to Figure 3, where we notice that the line profile of the [O I] 6363 line is rather complex and a kind of emission-like feature appears to exist (though not definite). Could it be an emission from the surrounding nebulosity, which, for example, was formed by mass ejection at the RGB phase in the past (recall that this is a horizontal-branch star)? Unfortunately, this line is too weak to make a definite argument even with this high S/N ratio, and it is also probable that what we see is nothing but noises. At any rate, we consider that Langer's (1991) mechanism may be worth further investigation. Such a dilution mechanism due to emission lines (if any exists) should be relatively more important for cases where the strength of the [O I] absorption line is intrinsically weak (i.e., more efficient for metal-poor case), which might explain the reason why the discordance is observed only in Population II stars (but not in Population I).

In addition, we should not forget the possibility that the effect of atmospheric inhomogeneity may cause appreciable discrepancies of abundances derived from different lines when analyzed classically, which can be tackled only by detailed realistic (2D or 3D) modeling of the atmosphere of metal-poor stars (e.g., Asplund et al. 1999).

4.5. Comparison with Other α -Elements

We thus conclude that [O/Fe] steadily increases from $\sim +0.6$ to $\sim +1.0$ as the metallicity becomes lower from [Fe/H] ~ -1.5 down to [Fe/H] ~ -3 .

Frankly speaking, however, this must be a rather embarrassing trend hard to interpret for theoreticians who are constructing models of Galactic nucleosynthesis history, because other α -elements (Mg, Si, Ca, Ti), which are believed to form in massive stars and ejected by type II SNe explosion like oxygen, generally show more or less the trend of flat “plateau” (i.e., $[\alpha/\text{Fe}] \sim 0.5$ at [Fe/H] ~ -3 ; cf. Fig. 2 in Ryan, Norris, & Beers 1996). This can be confirmed also from the results of Mg, Si, Ca, and Ti derived for our program stars (cf. Table 2). This would imply that some kind of unusual enrichment (e.g., pre-Galactic origin, or by supermassive stars) may have taken place for oxygen (while not for Mg, Si, Ca, and Ti) at the very early phase of the Galaxy, which would

have caused an exceptionally large [O/Fe] ratio at the old time of very low metallicity, though we are not qualified to state about wherether such a complicated modeling is possible or not.

Finally, we make one interesting remark concerning sulfur, another α -element which has not been well studied so far. According to our results given in Table 2, which were determined from only one S I line at 8694.63 Å, the [S/Fe] ratio shows a steeply increasing trend (from [S/Fe] \sim +0.3 at [Fe/H] \sim −1.5 to [S/Fe] \sim +1.1 at [Fe/H] \sim −2.7), which is similar to the tendency of [O/Fe] but not to that of [Mg/Fe], [Si/Fe], [Ca/Fe], and [Ti/Fe]. Although this kind of behavior for [S/Fe] (as well as for [O/Fe]) is not consistent with the current theoretical prediction (e.g., Timmes et al. 1995), their similarity may be worth attention, which might be a key to understanding the difference between these two groups of α -elements. More detailed analysis and discussion on S will be published in a separate paper (Takada-Hidai et al., in preparation).

5. CONCLUSIONS

We determined the oxygen abundance (along with the abundances of other elements) by a detailed non-LTE analysis for selected seven very metal-poor stars of $1/30 \sim 1/1000$ solar metallicity, based on the high-S/N spectra (in the red through near-IR region) observed with Keck HIRES, in order to study whether any significant systematic difference exist between the abundances derived from high-excitation O I permitted lines (7771–5, 8446) and those from low-excitation [O I] forbidden lines (6363, 6300).

The relatively hot ($T_{\text{eff}} = 5600$ K) horizontal-branch star HD 184266 turned out to be an interesting object, which shows markedly stronger O I permitted lines (7771–5, 8446) and very weak [O I] forbidden lines (6363, 6300). It revealed that the microturbulent velocity dispersion increases with height in the atmosphere of this star: this implies that one should take care about the choice of microturbulence in determining the abundance from saturated lines such as those permitted O I lines. Since the rather complex profile of [O I] 6363 line might be a sign of emission component (though not definite), Langer's (1991) hypothesis (dilution due to the “filled-in” emission from the circumstellar nebulosity) may deserve special attention as a possible weakening mechanism for this forbidden line.

We found that the both O I 7771–5 and O I 8446 yield quite consistent abundances with each other. On the other hand, the abundance determined from [O I] 6363 (or 6300) is generally lower typically by a few tenths dex than that derived from O I permitted lines, though the extent of the difference varies from star to star (two stars show a reasonable consistency).

The resulting [O/Fe] vs. [Fe/H] relation based on the permitted O I 7771–5 triplet shows a tight and clear tendency that [O/Fe] increases steadily from \sim +0.6 to \sim +1.0 as [Fe/H] decreases from \sim −1.5 down to \sim −3, which is quite similar to the trend found by the recent analyses of OH lines in UV (Israelian et al. 1998; Boesgaard et al. 1999). On the other hand, the [O/Fe] values derived from [O I] lines, which tend to be lower than the results of O I permitted lines by \sim 0.3

dex on the average, show a large diversity and considered to be unreliable compared to what was suggested from permitted O I lines.

Consequently, we would conclude that the most probable [O/Fe] vs. [Fe/H] relation at the very metal-deficient regime is the “steady increase” trend implied by O I permitted lines and OH lines in UV. We suspect that the [O I] forbidden lines tend to suffer with some kind of weakening, yielding an underestimated abundance, which becomes appreciable only in Population II metal-poor stars. Thus, according to our opinion, its use for abundance determination is questionable, in contrast to the general belief. All what we can state about the possible weakening mechanism is only speculative. Its cause might exist outer than the photosphere (e.g., nebulosity emission); alternatively, the photosphere itself might be responsible for the weakening (e.g., atmospheric inhomogeneity).

The [O/Fe] vs. [Fe/H] trend concluded in this paper can not be explained by the standard scenario of Galactic chemical evolution, since this does not conform to the tendency suggested from other well-studied α -elements such as Mg, Si, Ca, and Ti. According to the by-product of this study, however, sulfur (another α element) revealed an interesting behavior, in the sense that [S/Fe] shows a similar tendency to [O/Fe]. We hope that this observational implication will inspire the motivation of theoreticians toward a construction of better and realistic modeling of Galactic chemical evolution.

We are grateful to M. Kuchner for the reduction of the Keck HIRES data of CS 22892-052 as well as for putting the reduced spectrum at the authors’ disposal.

One of us (MTH) acknowledges the financial supports from grant-in-aid for the scientific research (A-2, No. 10044103) by Japan Society for the Promotion of Science as well as from grant-in-aid for research and education by Tokai University in the 1999 fiscal year, which enabled his observation with HIRES in 1999.

This research has made use of the SIMBAD database, operated at CDS, Strasbourg, France.

REFERENCES

Anders, E., & Grevesse, N. 1989, *Geochim. Cosmochim. Acta*, 53, 197

Asplund, M., Nordlund, Å., Trampedach, R., & Stein, R. 1999, *A&A*, 346, L17

Bessell, M. S., Sutherland, R. S., & Ruan, K. 1991, *ApJ*, 383, L71

Boesgaard, A. M., King, J. R., Deliyannis, C. P., & Vogt, S. S. 1999, *AJ*, 117, 492

Bond, H. E. 1980, *ApJS*, 44, 517

Carretta, E., Gratton, R. G., & Sneden, C. 2000, *A&A*, 356, 238

Cayrel de Strobel, G., Soubiran, C., Friel, E. D., Ralite, N., & François, P. 1997, *A&AS*, 124, 299

Fulbright, J. P., & Kraft, R. P. 1999, *AJ*, 118, 527

Gadun, A. S., & Ploner, S. R. O. 1999, *Kinematika Fiz. Nebesn. Tel.*, 15, 17

Gustaffson, B. 1999, in *Chemical Evolution from Zero to High Redshift* ed. J. R. Walsh & M. R. Rosa (Berlin, Springer), 1

Hauck, B., & Mermilliod, M. 1998, *A&AS*, 129, 431

Holweger, H., Kock, M., & Bard, A. 1995, *A&A*, 296, 233

Israelian, G., García López, R. J., & Rebolo, R. 1998, *ApJ*, 507, 805

Kurucz, R. L. 1993, Kurucz CD-ROM No.13 (Harvard-Smithsonian Center for Astrophysics)

Kurucz, R. L. 1995, Kurucz CD-ROM No.23 (Harvard-Smithsonian Center for Astrophysics)

Langer, G. E., 1991, *PASP*, 103, 177

McWilliam, A., Preston, G. W., Sneden, C., & Searle, L. 1995, *AJ*, 109, 2757

Mishenina, T. V., Korotin, S. A., Klochkova, V. G., & Panchuk, V. E. 2000, *A&A*, 353, 978

Pilachowski, C. A., Sneden, C., & Kraft, R. P. 1996, *AJ*, 111, 1689

Ryan, S. G., Norris, J. E., & Beers, T. C. 1996, *ApJ*, 471, 254

Sneden, C., Preston, G. W., McWilliam, A., & Searle, L. 1994, *ApJ*, 431, L27

Takeda, Y. 1992, *A&A*, 253, 487

Takeda, Y. 1995a, *PASJ*, 47, 287

Takeda, Y. 1995b, *PASJ*, 47, 463

Takeda, Y., Kawanomoto, S., & Sadakane, K. 1998a, PASJ, 50, 97

Takeda, Y., Kawanomoto, S., Takada-Hidai, M., & Sadakane, K. 1998b, PASJ, 50, 509

Takeda, Y., & Sadakane, K. 1997, PASJ, 49, 571

Timmes, F. X., Woosley, S. E., & Weaver, T. A. 1995, ApJS, 98, 617

Vogt, S. S. 1994, Proc. SPIE, 2198, 362

Table 1: OBSERVATIONAL DATA

| Star | <i>V</i> | Sp.Type | Date (UT) | No. of | | Total | R | S/N |
|-----------|----------|---------|----------------|----------|-------------|-------|---------|-----|
| | | | | Exposure | Exposure(s) | | | |
| HD 44007 | 8.06 | G5IV:w | 1999 Nov 11 | 3 | 900 | 60000 | 200-310 | |
| HD 84937 | 8.28 | sdF5 | 1999 Nov 9 | 3 | 900 | 60000 | 190-360 | |
| HD 88609 | 8.64 | G5IIIw | 1999 Nov 10 | 3 | 900 | 60000 | 230-340 | |
| HD 165195 | 7.34 | K3p | 1997 May 29-30 | 10 | 820 | 45000 | 370-510 | |
| HD 175305 | 7.20 | G5III | 1997 May 10 | 2 | 400 | 45000 | 410-660 | |
| HD 184266 | 7.57 | F2V | 1997 May 28 | 3 | 600 | 45000 | 330-550 | |

NOTE — Apparent visual magnitudes (*V*) and spectral types were taken from the SIMBAD database.

Table 2: ADOPTED MODEL PARAMETERS AND THE RESULTING ABUNDANCES

| Star | 44007 | 84937 | 88609 | 165195 | 175305 | 184266 | 22892-52 | Sun |
|---------------------------------|-------|-------|-------|--------|--------|--------|----------|------|
| T_{eff} (K) | 4850 | 6100 | 4500 | 4450 | 5100 | 5600 | 4760 | |
| $\log g$ (cm s^{-2}) | 2.00 | 4.00 | 1.00 | 1.10 | 2.50 | 1.70 | 1.30 | |
| [X] (metallicity) | -1.50 | -2.30 | -2.70 | -2.00 | -1.50 | -1.70 | -3.10 | |
| ξ (km s^{-1}) | 1.4 | 1.1 | 1.9 | 1.8 | 1.5 | 2.2 | 1.9 | |
| | | | | | | | | |
| C | 6.98 | 6.71 | 6.44 | 6.02: | 7.17 | 6.94 | ... | 8.56 |
| O | 7.96 | 7.51 | 7.01 | 7.52 | 7.80 | 7.92 | 7.02 | 8.93 |
| Na | ... | ... | ... | ... | ... | ... | 3.78 | 6.33 |
| Mg | 6.39 | 5.64 | 5.43 | 5.69 | 6.45 | 6.32 | 5.13 | 7.58 |
| Al | 4.67 | ... | ... | ... | ... | ... | ... | 6.47 |
| Si | 6.23 | 5.96 | 5.22 | 5.76 | 6.39 | 6.39 | ... | 7.55 |
| S | 5.92 | 5.87 | 5.60: | 5.68 | 6.07 | 5.98 | ... | 7.21 |
| K | ... | ... | ... | ... | ... | ... | 2.58 | 5.12 |
| Ca | 5.08 | 4.47 | 3.73 | 4.28 | 5.20 | 5.07 | 3.71 | 6.36 |
| Sc | 1.72 | ... | 0.22 | 1.21 | 1.94 | 1.61 | -0.10 | 3.10 |
| Ti | 3.51 | 3.37 | 2.37 | 2.94 | 3.83 | 3.47 | 2.25 | 4.99 |
| Cr | 3.97 | ... | 2.90 | 3.32 | 4.25 | 4.33 | 2.44 | 5.67 |
| Mn | 3.37 | ... | ... | ... | 4.06 | ... | ... | 5.39 |
| Fe | 5.94 | 5.34 | 4.79 | 5.46 | 6.18 | 5.94 | 4.61 | 7.51 |
| Co | 3.33 | ... | ... | 2.69 | 3.67 | ... | ... | 4.92 |
| Ni | 4.65 | 3.93 | 3.42 | 4.05 | 4.89 | 4.62 | 3.37 | 6.25 |
| Cu | 2.46 | ... | ... | 1.94 | 2.46 | ... | ... | 4.21 |
| Y | 0.63 | ... | ... | ... | 0.97 | ... | ... | 2.24 |
| Ba | 0.36 | -0.41 | -1.61 | 0.02 | 0.00 | 0.85 | 0.00 | 2.13 |
| La | -0.40 | ... | ... | -0.84 | ... | ... | ... | 1.22 |
| Eu | -1.13 | ... | ... | ... | ... | ... | ... | 0.51 |
| | | | | | | | | |
| [Fe/H] | -1.57 | -2.17 | -2.72 | -2.05 | -1.33 | -1.57 | -2.90 | |
| | | | | | | | | |
| [C/Fe] | -0.01 | 0.32 | 0.60 | -0.49: | -0.06 | -0.05 | ... | |
| [O/Fe] | 0.60 | 0.75 | 0.80 | 0.64 | 0.20 | 0.56 | 0.99 | |
| [Na/Fe] | ... | ... | ... | ... | ... | ... | 0.35 | |
| [Mg/Fe] | 0.38 | 0.23 | 0.57 | 0.16 | 0.20 | 0.31 | 0.45 | |
| [Al/Fe] | -0.23 | ... | ... | ... | ... | ... | ... | |
| [Si/Fe] | 0.25 | 0.58 | 0.39 | 0.26 | 0.17 | 0.41 | ... | |
| [S/Fe] | 0.28 | 0.83 | 1.11: | 0.52 | 0.19 | 0.34 | ... | |
| [K/Fe] | ... | ... | ... | ... | ... | ... | 0.36 | |
| [Ca/Fe] | 0.29 | 0.28 | 0.09 | -0.03 | 0.17 | 0.28 | 0.25 | |
| [Sc/Fe] | 0.19 | ... | -0.16 | 0.16 | 0.17 | 0.08 | -0.30 | |
| [Ti/Fe] | 0.09 | 0.55 | 0.10 | 0.00 | 0.17 | 0.05 | 0.16 | |
| [Cr/Fe] | -0.13 | ... | -0.05 | -0.30 | -0.09 | 0.23 | -0.33 | |
| [Mn/Fe] | -0.45 | ... | ... | ... | 0.00 | ... | ... | |
| [Co/Fe] | -0.02 | ... | ... | -0.18 | 0.08 | ... | ... | |
| [Ni/Fe] | -0.03 | -0.15 | -0.11 | -0.15 | -0.03 | -0.06 | 0.02 | |
| [Cu/Fe] | -0.18 | ... | ... | -0.22 | -0.42 | ... | ... | |
| [Y/Fe] | -0.04 | ... | ... | ... | 0.06 | ... | ... | |
| [Ba/Fe] | -0.20 | -0.37 | -1.02 | -0.06 | ... | 0.29 | ... | |
| [La/Fe] | -0.05 | ... | ... | -0.01 | ... | ... | ... | |
| [Eu/Fe] | -0.07 | ... | ... | ... | ... | ... | ... | |

NOTE — The solar abundances, with which stellar abundances are compared, were adopted from Anders & Grevesse (1989), except for that of Fe (7.51) which was taken from Holweger, Kock, & Bard (1995). Values with large uncertainties are indicated with colons (:).

Table 3: OXYGEN ABUNDANCE RESULTS DERIVED FROM VARIOUS LINES

| line | ξ (km s $^{-1}$) | W_λ (mÅ) | $\Delta \log \epsilon$ | $\log \epsilon$ | Δ_T | Δ_g | $\langle \log \epsilon \rangle_{7773}$ |
|--------------|-----------------------|------------------|------------------------|-----------------|------------|------------|--|
| HD 44007 | | | | | | | |
| 6363 | 1.4 | 4.0 | 0.00 | 7.67 | 0.05 | 0.13 | |
| 8446 | 1.4 | (18.5) | -0.10 | 7.98 | -0.17 | 0.11 | |
| 7772 | 1.4 | 20.3 | -0.14 | 7.88 | -0.18 | 0.11 | |
| 7774 | 1.4 | 19.0 | -0.13 | 7.99 | -0.18 | 0.11 | |
| 7775 | 1.4 | 13.8 | -0.12 | 8.01 | -0.16 | 0.11 | |
| | | | | | | | 7.96 |
| HD 84937 | | | | | | | |
| 6363 | 1.1 | ... | ... | ... | ... | ... | |
| 8446 | 1.1 | (15.6) | -0.07 | 7.50 | -0.12 | 0.10 | |
| 7772 | 1.1 | 19.2 | -0.10 | 7.45 | -0.11 | 0.10 | |
| 7774 | 1.1 | 17.1 | -0.09 | 7.54 | -0.11 | 0.10 | |
| 7775 | 1.1 | 11.5 | -0.08 | 7.55 | -0.11 | 0.10 | |
| | | | | | | | 7.51 |
| HD 88609 | | | | | | | |
| 6363 | 1.9 | 2.8 | 0.00 | 6.80 | 0.10 | 0.09 | |
| 8446 | 1.9 | ... | ... | ... | ... | ... | |
| 7772 | 1.9 | 4.6 | -0.10 | 7.13 | -0.19 | 0.12 | |
| 7774 | 1.9 | 2.0 | -0.09 | 6.89 | -0.19 | 0.12 | |
| 7775 | 1.9 | ... | ... | ... | ... | ... | |
| | | | | | | | 7.01 |
| HD 165195 | | | | | | | |
| 6363 | 1.8 | 10.9 | 0.00 | 7.47 | 0.05 | 0.13 | |
| 8446 | 1.8 | (3.7) | -0.07 | 7.38 | -0.22 | 0.11 | |
| 7772 | 1.8 | 7.3 | -0.09 | 7.44 | -0.20 | 0.12 | |
| 7774 | 1.8 | 5.0 | -0.09 | 7.40 | -0.20 | 0.13 | |
| 7775 | 1.8 | 6.3 | -0.10 | 7.73 | -0.20 | 0.12 | |
| | | | | | | | 7.52 |
| HD 175305 | | | | | | | |
| 6363 | 1.5 | 2.8 | 0.00 | 7.81 | 0.07 | 0.12 | |
| 8446 | 1.5 | (16.2) | -0.09 | 7.82 | -0.17 | 0.10 | |
| 7772 | 1.5 | 21.1 | -0.13 | 7.81 | -0.16 | 0.10 | |
| 7774 | 1.5 | 17.7 | -0.12 | 7.86 | -0.16 | 0.10 | |
| 7775 | 1.5 | 9.6 | -0.11 | 7.73 | -0.15 | 0.11 | |
| | | | | | | | 7.80 |
| HD 184266 | | | | | | | |
| 6363 | 2.2 | 1.3: | 0.00 | 7.47: | 0.10 | 0.09 | |
| 8446 | 2.2 | (109.0) | -0.26 | 8.06 | -0.14 | 0.12 | |
| 7772 | 2.2 | 106.8 | -0.46 | 8.17 | -0.13 | 0.10 | |
| 7774 | 2.2 | 90.1 | -0.36 | 8.16 | -0.13 | 0.10 | |
| 7775 | 2.2 | 62.5 | -0.30 | 8.06 | -0.13 | 0.11 | |
| 6363 | 5.1 | 1.3: | 0.00 | 7.47: | 0.10 | 0.09 | |
| 8446 | 5.1 | (109.0) | -0.23 | 7.98 | -0.13 | 0.11 | |
| 7772 | 5.1 | 106.8 | -0.29 | 7.92 | -0.13 | 0.11 | |
| 7774 | 5.1 | 90.1 | -0.27 | 7.94 | -0.12 | 0.11 | |
| 7775 | 5.1 | 62.5 | -0.22 | 7.91 | -0.12 | 0.11 | |
| | | | | | | | 7.92 |
| CS 22892-052 | | | | | | | |
| 6300 | 1.9 | 3.4: | 0.00 | 6.65: | 0.11 | 0.09 | |
| 6363 | 1.9 | 4.3: | 0.00 | 7.26: | 0.11 | 0.08 | |
| 7772 | 1.9 | 5.4 | -0.10 | 7.02 | -0.18 | 0.12 | |
| | | | | | | | 7.02 |

NOTE — The W_λ values for O I 8446 (blended with Fe I lines) presented here (with parentheses) were inversely computed from the abundances derived from profile-fitting, so that they may comprise the contribution of oxygen components only. $\Delta \log \epsilon$ (4th column) is the NLTE abundance correction ($\equiv \log \epsilon_{\text{NLTE}} - \log \epsilon_{\text{LTE}}$), while $\log \epsilon$ (5th column) is the NLTE abundance ($\log \epsilon_{\text{NLTE}}$). Δ_T and Δ_g (6th and 7th column) are the abundance variations in response to changes of $\Delta T = +150$ K and $\log g = +0.3$, respectively. $\langle \log \epsilon \rangle_{7773}$ is the mean NLTE abundance of the 7771–5 triplet averaged over each of the three components, which is the final oxygen abundance adopted in this paper. Regarding HD 184266, two set of results corresponding to two ξ values [2.2 km s $^{-1}$ (from Fe I lines) and 5.1 km s $^{-1}$ (from O I triplet)] are presented, though the latter set was used for calculating $\langle \log \epsilon \rangle_{7773}$. Values with large uncertainties are indicated with colons (:).

Fig. 1.— Spectrum portion comprising the O I 7771–5 triplet, where observed data are shown by circles. Solid lines indicate the theoretical spectra which were computed using the $\langle \log \epsilon_{7773} \rangle$ [mean abundance over each component of 7771–5 triplet; i.e., the finally adopted oxygen abundance in this paper (cf. Table 3)]. The positions of the component lines are indicated by arrows. An appropriate vertical offset is applied to each spectrum relative to the adjacent one.

Fig. 2.— Spectrum portion comprising the O I (+ Fe I) 8446 feature. Observed data are shown by circles. Solid lines are the theoretical spectra corresponding to $\langle \log \epsilon_{7773} \rangle$ as in Figure 1.

Fig. 3.— Spectrum portion at the forbidden line [O I] 6363, where observed data are shown by circles. (For CS 22892-052, the portion of [O I] 6300 is additionally shown in the inset.) The theoretical spectra corresponding to the adopted oxygen abundance ($\langle \log \epsilon_{7773} \rangle$) are shown by solid lines as in Figure 1.

Fig. 4.— Comparison of the adopted oxygen abundance derived from O I 7771–5 ($\langle \log \epsilon_{7773} \rangle$) with that of O I 8446 or [O I] 6363 (6300). Parenthesized symbols indicate the data with large uncertainties.

Fig. 5.— [O/Fe] vs. [Fe/H] correlation resulting from the present analysis (the circles represent our O I 7771-5 results finally adopted, while crosses represent the [O I] results), overplotted on the relation derived by Israelian et al. (1998) based on the OH lines in UV (triangles). Parenthesized symbols are uncertain values.

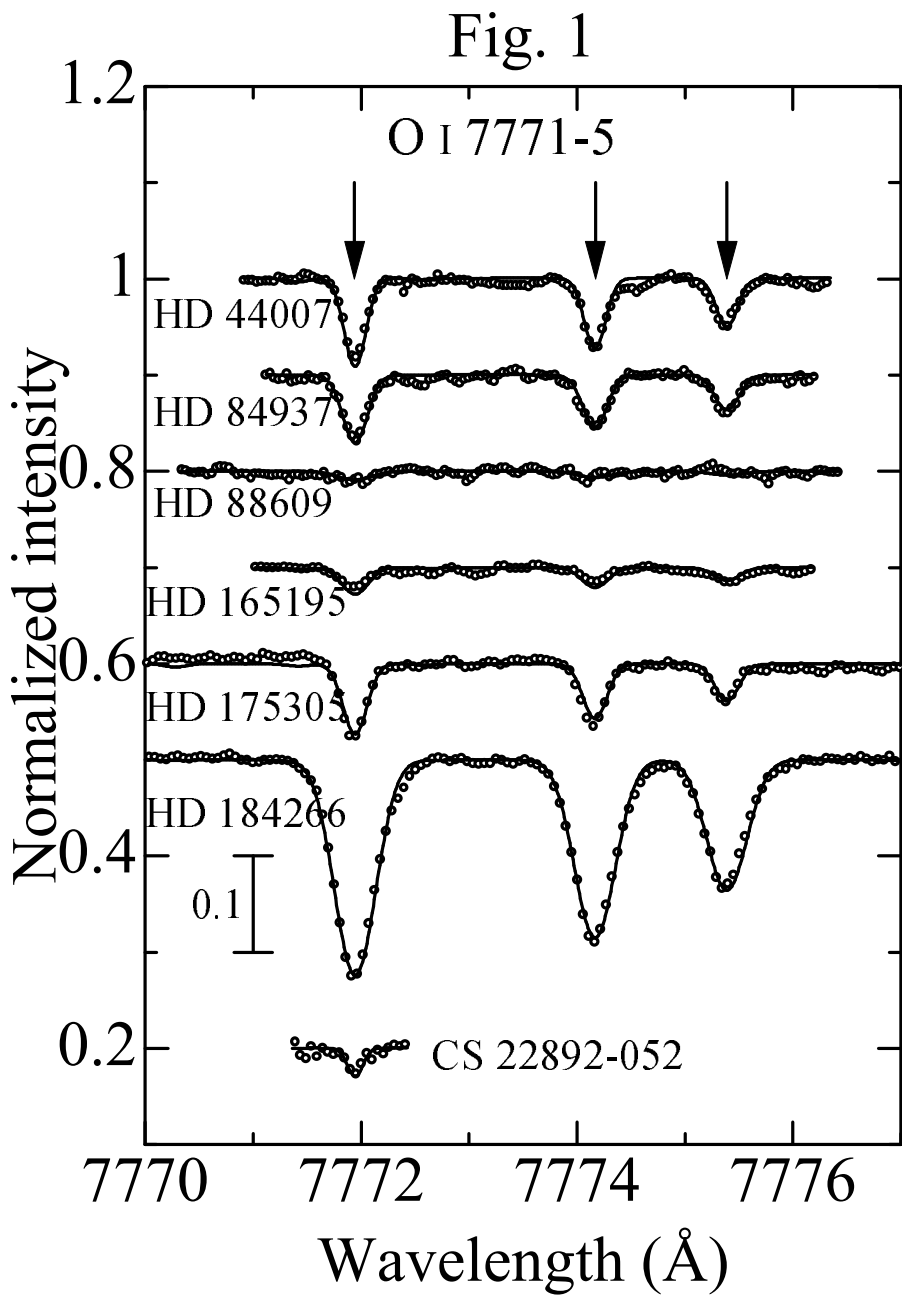


Fig. 2

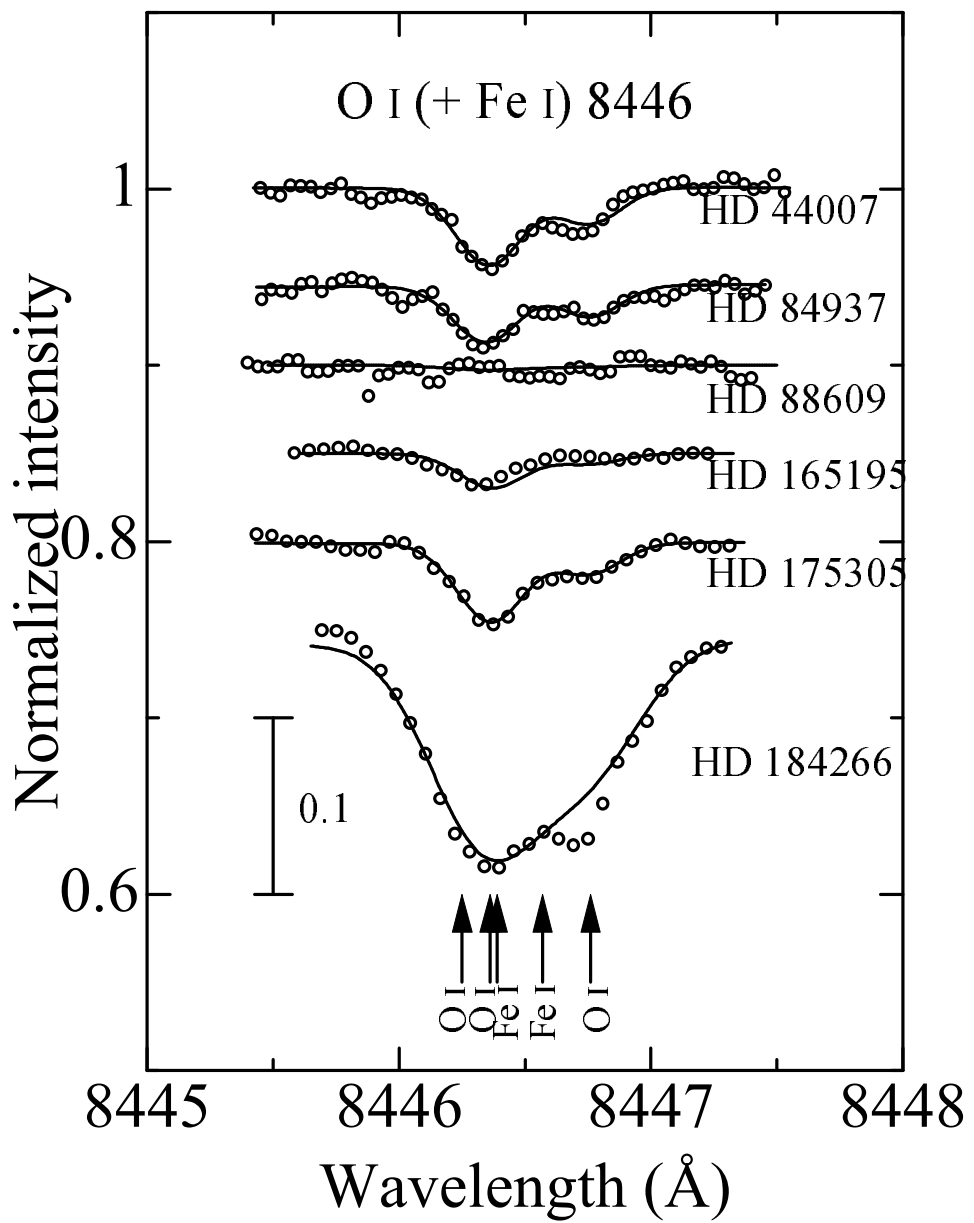


Fig. 3

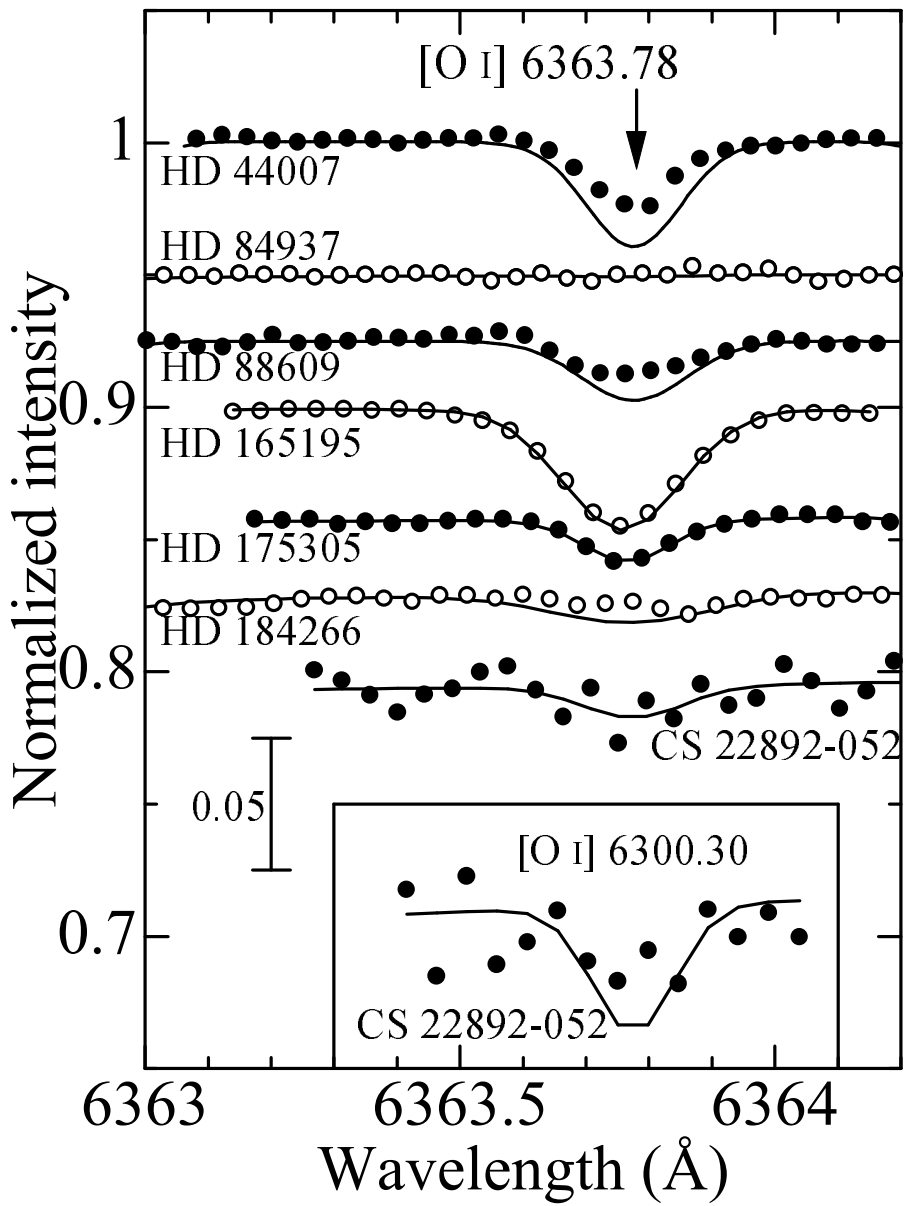


Fig. 4

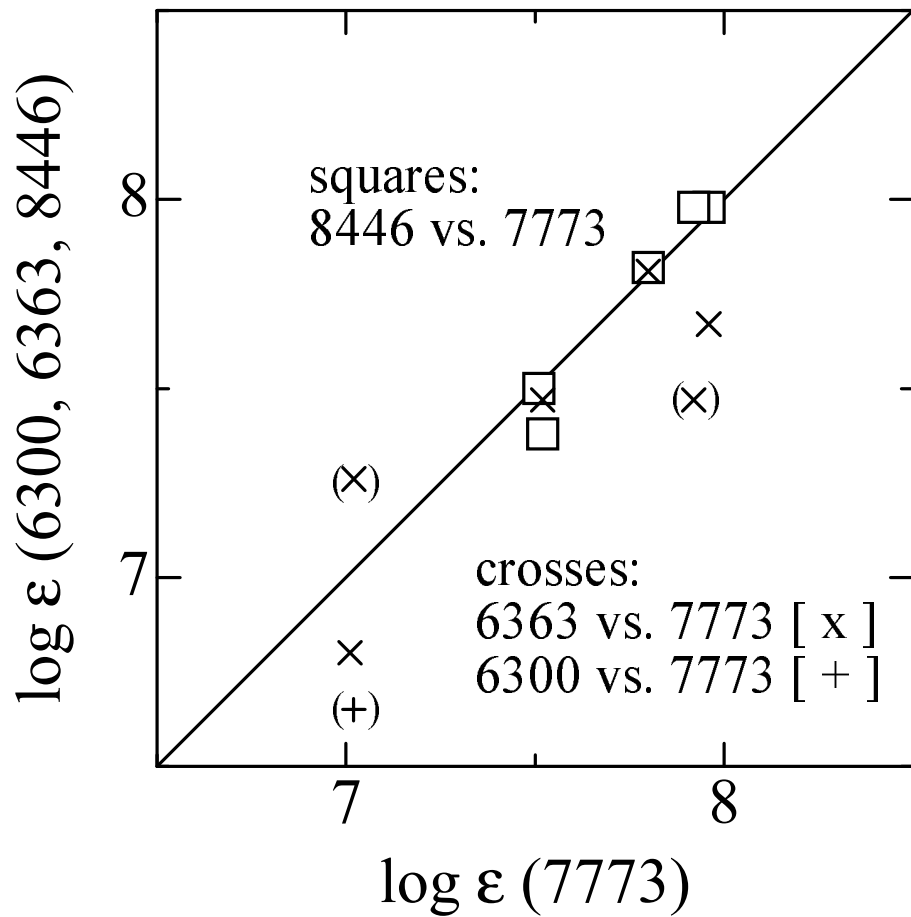


Fig. 5

